Hindawi
International Journal of Antennas and Propagation
Volume 2019, Article ID 9106749, 8 pages
https://doi.org/10.1155/2019/9106749

Research Article

DOA Estimation Performance Analysis and Verification of Dual Crossed-Loop/Monopole Antenna Array

Sijie Wang, Biyang Wen, and Yingwei Tian

Electronic Information School of Wuhan University, Wuhan 430072, China

Correspondence should be addressed to Biyang Wen; bywen@whu.edu.cn

Received 27 May 2019; Revised 3 August 2019; Accepted 27 August 2019; Published 16 September 2019

Academic Editor: Paolo Baccarelli

The compact high-frequency surface wave radar using a crossed-loop/monopole (CLM) antenna as the receiving sensor has been widely used in ocean remote sensing and target monitoring. However, the direction of arrival (DOA) estimation accuracy of a single CLM antenna is the dominant factor that restricts the target monitoring performance of the compact HF radar. Besides, the single CLM antenna can estimate two signals simultaneously at most, but its effectiveness is challenged by the pattern distortion and the existence of coherent sources, which limits the application range of the compact HF radar. In this study, a compact array combining two CLM antennas is proposed to improve the DOA estimation accuracy and solve the multisource DOA estimation problem. The estimation error and multisource DOA estimation performance of a dual CLM antenna array are analyzed by formula derivation and simulation. Furthermore, the field experiment results are given to demonstrate the performance improvement of the dual CLM antenna array.

1. Introduction

By using the vertical polarization electromagnetic wave that travels along the curvature of ocean surface with low loss, the high-frequency surface wave radar (HFSWR) can be used for real-time ocean remote sensing over the horizon range, including not only the measurement of ocean surface dynamic parameters [1, 2] but also the detection and tracking of targets [3, 4]. According to the antenna type, the HF radar can be divided into two types: the phased array system [5] and the CLM antenna system [6, 7]. The CLM antenna consists of three elements, including an omnidirectional monopole and two cross-placed loops, which are named as loop B and loop A [8]. The development of the CLM antenna enables the HF radar to be used at some scenarios without requiring a large antenna field, which also reduces the installation and maintenance costs.

However, the compact HF radar with the single CLM antenna has some defects in practical application. Firstly, the excessive DOA estimation error caused by antenna pattern distortion in practice significantly reduces the performance of sea-state remote sensing [9] and hard target tracking [10]. The CLM antenna can achieve DOA estimation by using the multisignal classification (MUSIC) algorithm [11, 12] for direction finding, but since the MUSIC algorithm requires antenna pattern information, the unavoidable distortion of antenna pattern can easily cause DOA estimation errors [13]. Although many methods of calibration and pattern measurement have been proposed [14–16], the DOA estimation accuracy still limits the performance of hard target detection and tracking. Furthermore, a machine learning algorithm [17] has been proposed recently and has achieved good performance, but the algorithm relies on a large amount of data for training. Moreover, a CL processing method [18] applied to the CLM antenna has also been proposed to avoid the complexity of measuring antenna pattern, but the improvement of the algorithm is limited. Secondly, a single CLM antenna with three elements is challenged in the case of multisource DOA estimation. Although a single CLM antenna can theoretically distinguish two signal sources, the multisource estimation problem is still difficult to solve due to the antenna pattern distortion and the existence of coherent sources. For an HF radar with the range resolution of kilometers, a range-Doppler (RD)

unit containing two or more signals from ocean echoes or vessel targets is a possible event, especially when the application environment has a 360-degree look angle, such as floating platforms and offshore drilling platforms. This case will lead to the problem of coherent signal estimation, but the decoherence algorithm applied to the single CLM antenna has not been explored yet.

An effective way is using a dual CLM antenna array as the receiving sensor to solve the aforementioned problems while retaining the advantage of its small size. In this study, the DOA estimation performance of the dual CLM antenna array is investigated. The estimation error of the dual CLM antenna array based on the MUSIC algorithm is theoretically derived. Then, simulations are conducted to analyze the multisource DOA estimation performance. The estimation results of field experimental data are given to prove that the DOA estimation accuracy of the dual CLM antenna array is higher than that of the single CLM antenna, which is consistent with the theoretical formula. Moreover, a multisource case of vessel targets in the shore-based HF radar data is studied, the result also confirms that it is effective to estimate the DOAs of multisource with dual CLM antenna array.

This article is organized as follows. Section 2 analyzes the estimation error and multisource DOA estimation performance of the dual CLM antenna array by theoretical derivation and simulation. Section 3 gives the experimental results. Section 4 contains a brief conclusion.

2. Analysis of DOA Estimation Performance

2.1. MUSIC Algorithm and Estimation Error. In the case of single signal source, the signal model can be written as

$$\mathbf{x}(t) = \mathbf{a}(\theta)s(t) + \mathbf{n}(t), \tag{1}$$

where $\mathbf{x}(t) = [x_1(t), x_2(t), \ldots, x_m(t)]^T$ is the received data vector of size $m \times 1$, m is the number of array elements, $s(t)$ is the echo signal, $\mathbf{a}(\theta) = [a_1(\theta), a_2(\theta), \ldots, a_m(\theta)]^T$ is the steering vector of array, and $\mathbf{n}(t) = [n_1(t), n_2(t), \ldots, n_m(t)]^T$ is the white noise. The covariance matrix of received data can be decomposed into signal part and noise part, which can be expressed as

$$\mathbf{R} = E\left[\mathbf{x}(t)\mathbf{x}^H(t)\right] = \mathbf{a}(\theta)R_S\mathbf{a}^H(\theta) + \sigma^2\mathbf{I}, \tag{2}$$

where $R_S = E[s(t)s^*(t)]$, σ^2 is the variance of noise, and $(\cdot)^*$ and $[\cdot]^H$ represent conjugate and conjugate transpose operation, respectively. Eigen decomposition of $\mathbf{R}$ can be written as

$$\mathbf{R} = \mathbf{U}_S\sum_S \mathbf{U}_S^H + \mathbf{U}_N\sum_N \mathbf{U}_N^H, \tag{3}$$

where $\mathbf{U}_S$ represents signal subspace formed by eigenvectors corresponding to large eigenvalues and $\mathbf{U}_N$ represents the noise subspace formed by eigenvectors corresponding to small eigenvalues. Ideally, the steering vector of signal subspace is orthogonal to the noise subspace, viz., $\mathbf{a}^H(\theta)\mathbf{U}_N = 0$. DOA estimation based on the MUSIC algorithm is achieved by finding the $\widehat{\theta}$ that minimizes $\mathbf{a}^H(\theta)\mathbf{U}_N\mathbf{U}_N^H\mathbf{a}(\theta)$, which can be expressed as

$$\widehat{\theta} = \arg_\theta \min \mathbf{a}^H(\theta)\mathbf{U}_N\mathbf{U}_N^H a(\theta). \tag{4}$$

The steering vector of a CLM antenna with the normal direction of 0° can be written as

$$\mathbf{a}_c(\theta) = \left[1,\ \cos\left(\theta + \frac{\pi}{4}\right),\ \sin\left(\theta + \frac{\pi}{4}\right)\right]^T. \tag{5}$$

The dual CLM antenna array is a combination of uniform linear array (ULA) and CLM antenna, as shown in Figure 1. Therefore, when the normal directions of CLM antennas and the array are both 0°, its steering vector can be expressed as

$$\mathbf{a}_d(\theta) = \left[1,\ \cos\left(\theta + \frac{\pi}{4}\right),\ \sin\left(\theta + \frac{\pi}{4}\right), e^{j\varphi(\theta)}, \ldots, e^{j\varphi(\theta)} \cdot \cos\left(\theta + \frac{\pi}{4}\right), e^{j\varphi(\theta)} \cdot \sin\left(\theta + \frac{\pi}{4}\right)\right]^T, \tag{6}$$

where $\varphi(\theta) = -2\pi d \cdot \sin\theta/\lambda$ is the phase shift, d is the spacing of adjacent elements, and λ is the wavelength.

Stoica and Nehorai [19] have proved that the estimation error of the MUSIC algorithm obeys the Gaussian distribution whose mean is zero, and its variance can be written as

$$\begin{aligned}\mathrm{var}(\widehat{\theta}) &= E\left[(\widehat{\theta} - \theta)^2\right] \\ &= \frac{1}{2N \cdot \mathrm{SNR}}\left[1 + \frac{(a^H(\theta)a(\theta))^{-1}}{\mathrm{SNR}}\right]\frac{1}{h(\theta)},\end{aligned} \tag{7}$$

where N is the number of snapshots and SNR is the signal-to-noise ratio of samples. $h(\theta)$ can be written as

$$h(\theta) = \mathbf{d}^H(\theta)\left[I - \mathbf{a}(\theta)\left(\mathbf{a}^H(\theta)\mathbf{a}(\theta)\right)^{-1}\mathbf{a}^H(\theta)\right]\mathbf{d}(\theta), \tag{8}$$

where $\mathbf{d}(\theta)$ is the derivative of $\mathbf{a}(\theta)$ to θ, viz., $\mathbf{d}(\theta) = d[\mathbf{a}(\theta)]/d\theta$.

For an idealized CLM antenna, the MUSIC error variance has been deduced by [20] and can be expressed as

$$\mathrm{var1}(\widehat{\theta}) = \frac{1}{2N \cdot \mathrm{SNR}} \cdot \left(1 + \frac{1}{2\mathrm{SNR}}\right). \tag{9}$$

Similarly, the MUSIC error variance of the dual CLM antenna array can be expressed as

$$\mathrm{var2}(\widehat{\theta}) = \frac{1}{2N \cdot \mathrm{SNR}} \cdot \left(1 + \frac{1}{4\mathrm{SNR}}\right) \cdot \frac{1}{2 + (2\pi d\cos\theta/\lambda)^2}. \tag{10}$$

Comparing (9) and (10), $\mathrm{var2}(\widehat{\theta})$ is always less than $\mathrm{var1}(\widehat{\theta})$ with the same N and SNR values. Figure 2 shows the theoretical MUSIC error of different antenna types when $N = 100$, the incident angle equals 0° and the spacing of adjacent array elements is set as half of the wavelength. From this figure, it is seen that the MUSIC performance of the dual CLM antenna array is superior to that of the single CLM antenna and close to that of the three-elements ULA. But the

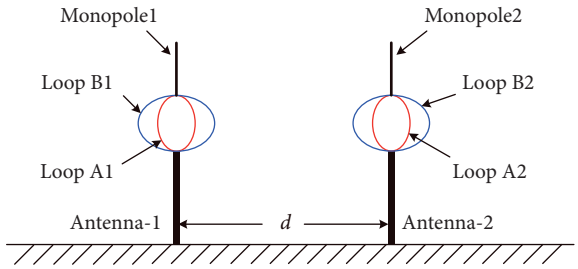

Figure 1: Diagram of a dual CLM antenna array, where monopole, loop B, and loop A are the three elements of the single CLM antenna, and d is the spacing between two CLM antennas.

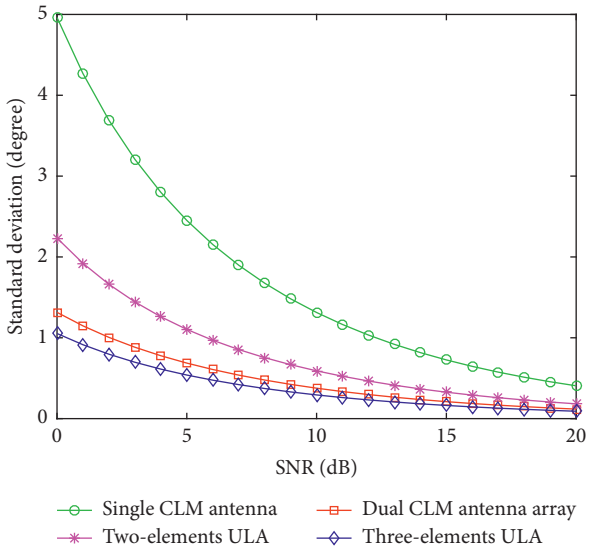

Figure 2: Theoretical MUSIC error of different antenna types. For the dual CLM array and ULAs, the array spacing is set as half-wavelength.

differences between the antennas decrease with the increase of SNR.

2.2. Analysis of Two-Sources DOA Estimation Performance. According to [21], there are only phase delay and amplitude weighting between the coherent signals, i.e., the frequencies of two coherent signals are the same. Conversely, the two signals are incoherent signals when they have different frequencies. For two coherent signals coming from θ_1 and θ_2, we can rewrite (1) as

$$\mathbf{x}(t) = \mathbf{A}(\theta)\mathbf{s}(t) + \mathbf{n}(t), \tag{11}$$

where $\mathbf{s}(t) = [s_1(t), s_2(t)]^T = [s_1(t), \alpha \cdot s_1(t)]^T$, in which α is the complex scalar describing the gain and phase relationship between the two coherent signals, and $\mathbf{A}(\theta) = [\mathbf{a}(\theta_1), \mathbf{a}(\theta_2)]$. Notice that $\mathbf{R}_s = E[\mathbf{s}(t)\mathbf{s}^H(t)]$ is singular and the rank of $\mathbf{R}_s$ is 1 when the signals are coherent. Obviously, the rank of $\mathbf{R}$ also drops to 1, i.e., the dimension of the signal subspace is less than the number of signal sources, so the accurate DOA estimation cannot be achieved. To solve this problem, decorrelate processing is needed to restore the nonsingularity of $\mathbf{R}$. The forward spatial smoothing algorithm [22] is a typical decorrelate algorithm. The principle of the algorithm is to divide the receiving antenna array into several subarrays, then use the covariance matrices of data received by subarrays to obtain the modified nonsingular covariance matrix. The robustness of this algorithm comes at the expense of a reduced effective aperture. Besides, the algorithm requires that the number of subarrays must be greater than or equal to the number of signal sources, and the size of each subarray must be greater than the number of signal sources. Obviously, the algorithm cannot be applied to the single CLM antenna since it does not meet the latter requirement. For the dual CLM antenna array using the algorithm, two CLM antennas can be regarded as two subarrays, then the modified covariance matrix can be expressed as

$$\mathbf{R}_f = \frac{\mathbf{R}_1 + \mathbf{R}_2}{2} = \frac{E[\mathbf{x}_1(t)\mathbf{x}_1^H(t)] + E[\mathbf{x}_2(t)\mathbf{x}_2^H(t)]}{2}, \tag{12}$$

where $\mathbf{x}_1(t)$ and $\mathbf{x}_2(t)$ are the received data of antenna-1 and antenna-2, respectively. The covariance matrix $\mathbf{R}_f$ is substituted into (3) and (4) to achieve the DOA estimation of coherent signals.

To analyze the multisource DOA estimation performance of the dual CLM antenna array under the incoherent and coherent conditions, Monte Carlo simulations are carried out in this section. The simulation parameters are as follows: the number of snapshots is 30, and the snapshots are statistically independent, the number of independent trial times is 500, and the spacing of adjacent elements is half of the wavelength.

Figure 3 shows the MUSIC spectrum of the dual CLM antenna array at different SNRs in the incoherent and coherent cases. It is seen that the spectral peak in the incoherent case is sharper than that in the coherent case when the SNRs of signals are equal. With the decrease of the SNR, the peak outlines of both cases are gradually smoothed. When the SNR is equal to 15 dB, the spectral peaks can hardly be distinguished in the coherent case, while the two spectral peaks can still be clearly discernible in the incoherent case. The results show that the spatial smoothing algorithm can achieve the DOA estimation of coherent signals, but the estimation performance in the coherent case is worse than that in the incoherent case.

In our simulations, we define two signals coming from θ_1 and θ_2, and the corresponding DOA estimation results are $\widehat{\theta}_1$ and $\widehat{\theta}_2$. The power of two signals is equivalent. Here, the trial is considered as a successful estimation if $|\widehat{\theta}_1 - \theta_1| \leq 5^\circ$ and $|\widehat{\theta}_2 - \theta_2| \leq 5^\circ$. Figure 4(a) shows the probability of successful estimation under different SNRs at the incident angles of 0° and 40°. As can be seen from the figure, a higher SNR (approximately 15 dB) is required for the coherent case to achieve the same estimation performance as in the incoherent condition.

In Figure 4(b), we set $\theta_1 = 0^\circ$ and change the value of θ_2 to show the DOA estimation performance at different angular separations when SNR = 20 dB. It can be observed that the estimation performance in the incoherent case is superior to that of the coherent case when the incident angles of two signals are close. On the other hand, when the SNR is

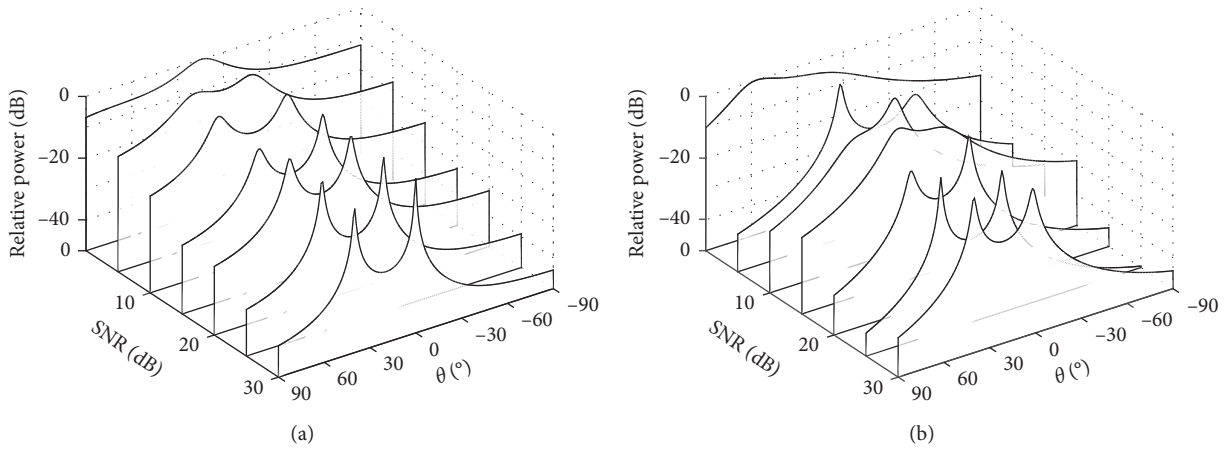

FIGURE 3: MUSIC spectrum of the dual CLM antenna array versus the SNR with incident angles of 0° and 40°. (a) Incoherent signals. (b) Coherent signals.

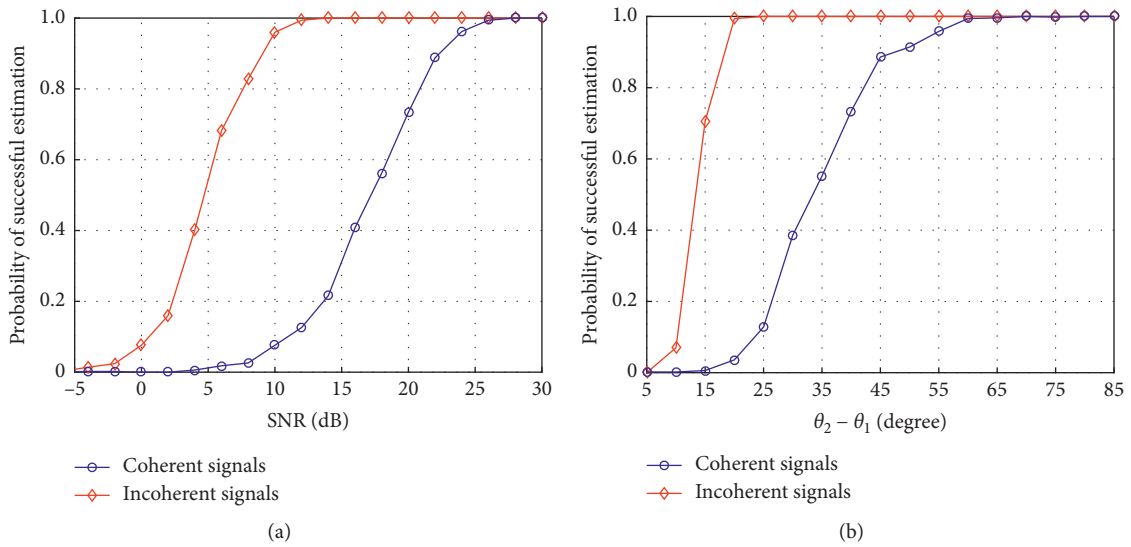

FIGURE 4: Simulation results of the successful estimation probability in incoherent and coherent cases. (a) Probability of successful estimation versus the SNR with incident angles of 0° and 40°. (b) Probability of successful estimation versus incident angles when SNR = 20 dB.

set as 20 dB, the two signals with an angular deviation greater than 25° can be accurately estimated in the incoherent case, but the angular deviation is required to be greater than 65° in the coherent case. On the other hand, these simulation results also provide the theoretical basis for the actual estimation ability of the compact HF radar under different conditions.

3. Field Experiment and Results

In order to validate the experimental performance of the dual CLM antenna array, a field experiment was carried out at Longhai (24.27°N, 118.14°E) in Fujian, China. The compact radar system used in the field experiment is OSMAR-SD [23] developed by the Radar and Signal Processing Laboratory, Wuhan University. The radar works at 13.05 MHz with a bandwidth of 60 kHz which theoretically produced a 2.5 km range resolution. The receiving antenna system is a dual CLM antenna array with a spacing of 14 m between the two CLM antennas. In addition, an Automatic Identification System (AIS) receiver is installed at the radar site to receive the information broadcast by vessels equipped with an AIS transmitter. The AIS information provides characteristics of vessels including Maritime Mobile Service Identify (MMSI), location, velocity, and so on.

3.1. Comparison of DOA Estimation Accuracy. The constant false-alarm-rate (CFAR) algorithm [24] is used here to detect the targets in the RD spectrum, and the data received by the two CLM antennas are processed separately. The location, velocity, and heading of the vessel reported by the AIS are converted to range, radial velocity, and azimuth under the radar coordinate. Then, the intersection of detection results of the two CLM antennas is matched with the AIS-reported vessels by using an empirical strategy of a two-

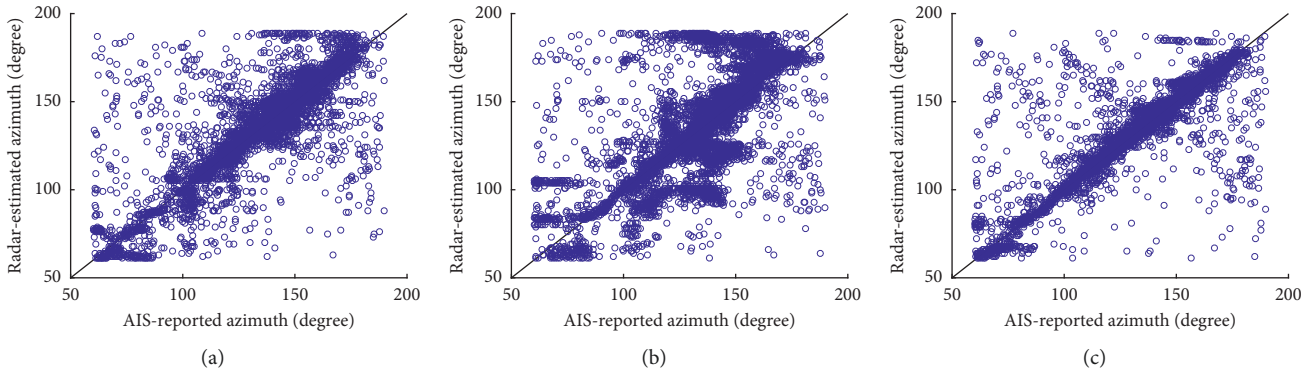

Figure 5: DOA estimation results in Longhai. (a) Antenna-1. (b) Antenna-2. (c) Dual antenna array.

dimensional threshold, that is, if the distance between the detected target and the AIS-reported vessels is within a range bin and the velocity difference is less than two Doppler bins, the target pairs are recognized to be matched. The matched targets are used for DOA estimation and the corresponding vessel azimuths calculated from AIS information are used as ground truth information. It should be noted that a sliding window method [7] is used to form snapshots for the MUSIC algorithm since OSMAR-SD is a coherent Doppler radar.

Figure 5 shows the DOA estimation results, where the horizontal axis represents the azimuth information reported by the AIS, the vertical axis represents the radar estimated results and the black line represents the ideal estimation. The number of data point is 7559. Apparently, the results of the dual antenna array are more concentrated around the black line, which means that the estimations of the dual antenna array are closer to the real values. The comparison of correlation coefficients and root-mean-square errors (RMSEs) between the estimated results and AIS-reported results shown in Table 1 also proves that the dual CLM antenna array has higher estimation accuracy.

Figure 6 shows the error distribution of DOA estimation results. It is obvious that the error distribution curve of the dual CLM antenna array is narrower and more concentrated on zero. The proportions of samples whose absolute error is less than 5° are also shown in the figure. The proportions responsible for two CLM antennas are 0.802 and 0.557, respectively, and the proportion of the dual CLM antenna array is 0.906. The increase of the proportion also indicates the performance improvement of the dual CLM antenna array.

Figure 7 shows the estimation errors of the single antenna and the dual antenna array associated with SNRs, where the dotted lines represent the theoretical values, and the solid lines represent the error values obtained by statistically calculating the estimation results of experimental data. The experimental results of the single antenna and the dual antenna array are both obtained by employing the MUSIC algorithm with the measured pattern. It is seen that the processing results of experimental data are similar to the theoretical curves, and the trends of curves are consistent. This figure also verifies that the estimation performance of

Table 1: Statistics of DOA estimation results.

	Antenna-1	Antenna-2	Dual antenna array
Corr. coef	0.816	0.663	0.845
RMSE (degree)	14.96	23.51	13.27

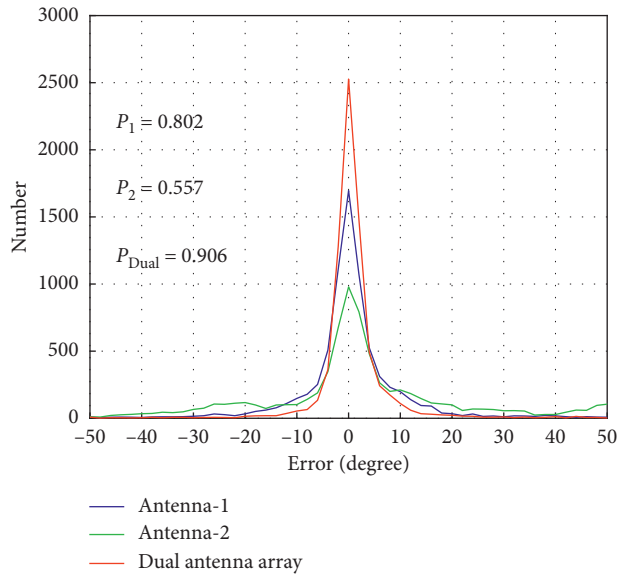

Figure 6: The error distribution of DOA estimation results.

the dual CLM antenna array is better, especially when the SNR is relatively low. However, the results of experimental data show higher error values than the theoretical curves. The cause of this difference may be pattern distortion and the measurement error of antenna pattern. The pattern distortion may cause the experimental estimation error to deviate from the results obtained from (9) and (10), and the measurement error between measured pattern and actual pattern may also cause this difference.

3.2. Results of Two-Sources DOA Estimation. Figure 8 shows a coherent case of multisource in experimental data. In Figure 8(a), there is an RD unit containing two vessel targets according to the AIS reports. The azimuths of the two vessels

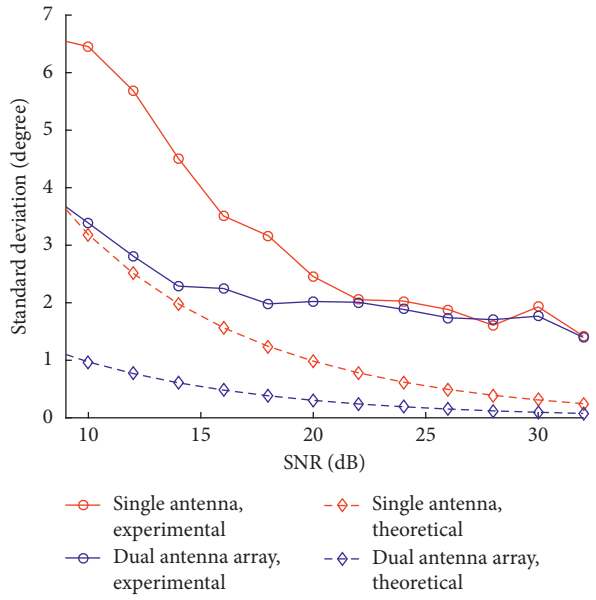

Figure 7: Comparison of simulated and experimental DOA estimation errors at different SNRs. The incident azimuth of the signal is −20°.

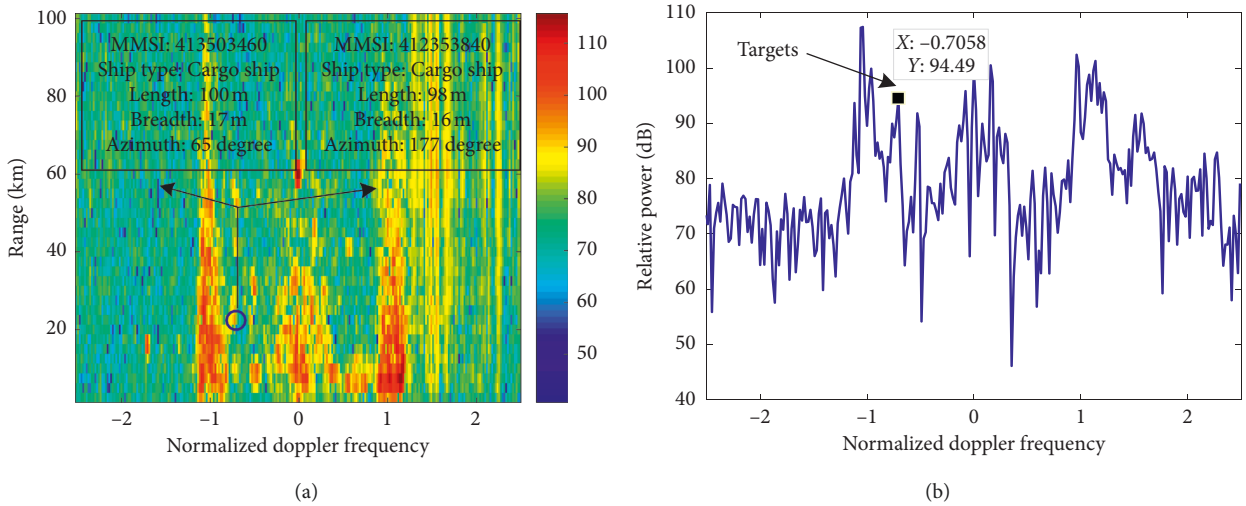

Figure 8: A case of multisources with target azimuths of 65° and 177°. (a) RD spectra. (b) Doppler spectra at the 9th range bin (22.5 km). Color bar in (a) is used to illustrate the signal strength in dB.

are 65° and 177°, respectively. The MMSI and static information (size and ship type) of vessels are also shown in the figure. It is seen from Figure 8(b) that a strong peak appears at the Doppler frequency point reported by the AIS, which is the echo signal of vessel targets.

Figure 9 shows the normalized MUSIC spectrum of multisource DOA estimation, where the result of the dual antenna array is obtained by applying the forward spatial smoothing algorithm, and the results of antenna-1 and antenna-2 are obtained by the traditional MUSIC algorithm. It can be observed that only one dominant peak responding to the azimuth of the second vessel target is shown in the spectrum of two CLM antennas, and the peak in the spectrum of antenna-1 deviates significantly from the actual azimuth value. However, the MUSIC spectrum of the dual CLM antenna array shows two peaks at 66° and 177°, which is consistent with the actual azimuth of targets. This estimation results indicate the defect of the single CLM antenna that it cannot achieve the multisource estimation. It also verifies the feasibility of using the dual CLM antenna array to estimate the DOAs of multisource. On the other hand, based on the simulation results in the previous section, it can be reasonably inferred that the dual CLM antenna array will have better performance under the incoherent case in practical applications. However, since only shore-based radar data are available for analysis now, the experimental performance varying with the SNR and angular separation is expected to be discussed after obtaining more abundant data, such as platform-mounted radar data.

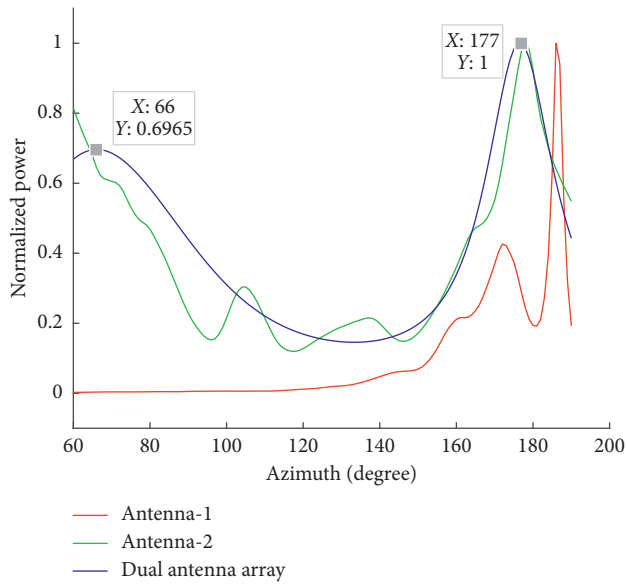

Figure 9: Normalized MUSIC spectrum of targets with actual azimuths of 65° and 177°.

4. Conclusion

In this article, we propose to use the dual CLM antenna array as the receiving sensor of the HF radar to improve the DOA estimation accuracy and solve the multisource DOA estimation problem. The DOA estimation accuracy and multisource estimation performance of the dual CLM antenna array are studied by formula derivation and simulations. The estimation results of thousands of detected samples prove that the dual CLM antenna array has higher estimation accuracy than the single CLM antenna. The estimation error of experimental data is also consistent with the theoretical curve. A multisource case in shore-based radar data is investigated, and the result verifies that the dual CLM antenna array can achieve multisource DOA estimation while the single CLM antenna fails. This improvement extends the application range of the compact HF radar and makes it possible to install the radar in the environment such as the floating platform.

Data Availability

The data used to support the findings of this study are available from the corresponding author upon request.

Conflicts of Interest

The authors declare that there are no conflicts of interest regarding the publication of this paper.

Acknowledgments

This work was supported by the National Natural Science Foundation of China (Grant nos. 61671331, 41706200, and 61661009), the National Key R&D Program of China (Grant no. 2017YFC0405703), the Fundamental Research Funds for the Central Universities (Grant no. 2042018kf1009), and the Natural Science Foundation of Jiangsu Province (Grant no. SBK2019040262).

References

[1] D. E. Barrick, "Extraction of wave parameters from measured HF radar sea-echo doppler spectra," *Radio Science*, vol. 12, no. 3, pp. 415–424, 1977.

[2] W. Huang, E. Gill, X. Wu, and L. Li, "Measurement of sea surface wind direction using bistatic high-frequency radar," *IEEE Transactions on Geoscience and Remote Sensing*, vol. 50, no. 10, pp. 4117–4122, 2012.

[3] R. Khan, B. Gamberg, D. Power et al., "Target detection and tracking with a high frequency ground wave radar," *IEEE Journal of Oceanic Engineering*, vol. 19, no. 4, pp. 540–548, 1994.

[4] S. Maresca, P. Braca, J. Horstmann, and R. Grasso, "Maritime surveillance using multiple high-frequency surface-wave radars," *IEEE Transactions on Geoscience and Remote Sensing*, vol. 52, no. 8, pp. 5056–5071, 2014.

[5] K.-W. Gurgel, G. Antonischki, H.-H. Essen, and T. Schlick, "Wellen radar (WERA): a new ground-wave HF radar for ocean remote sensing," *Coastal Engineering*, vol. 37, no. 3-4, pp. 219–234, 1999.

[6] B. J. Lipa and D. E. Barrick, "Least-squares methods for the extraction of surface currents from CODAR crossed-loop data: application at ARSLOE," *IEEE Journal of Oceanic Engineering*, vol. 8, no. 4, pp. 226–253, 1983.

[7] H. Zhou and B. Wen, *Portable High Frequency Surface Wave Radar OSMAR-S*, Springer International Publishing, Cham, Switzerland, 2015.

[8] A. R. Carr, "Three-element antenna formed of orthogonal loops mounted on a monopole," US Patent 4,433,336, 1984.

[9] K. Laws, J. D. Paduan, and J. Vesecky, "Estimation and assessment of errors related to antenna pattern distortion in CODAR SeaSonde high-frequency radar ocean current measurements," *Journal of Atmospheric and Oceanic Technology*, vol. 27, no. 6, pp. 1029–1043, 2010.

[10] H. J. Roarty, M. Smith, S. M. Glenn et al., "Expanding maritime domain awareness capabilities in the arctic: high frequency radar vessel-tracking," in *Proceedings of the 2013 IEEE Radar Conference (RadarCon13)*, Ottawa, Canada, April 2013.

[11] R. Schmidt, "Multiple emitter location and signal parameter estimation," *IEEE Transactions on Antennas and Propagation*, vol. 34, no. 3, pp. 276–280, 1986.

[12] D. E. Barrick and B. J. Lipa, "Radar angle determination with MUSIC direction finding," US Patent 5,990,834, 1999.

[13] T. M. Cook, T. DePaolo, and E. J. Terrill, "Estimates of radial current error from high frequency radar using MUSIC for bearing determination," in *Proceedings of the IEEE Oceans*, Vancouver, Canada, September 2007.

[14] B. M. Emery, L. Washburn, C. Whelan, D. Barrick, and J. Harlan, "Measuring antenna patterns for ocean surface current HF radars with ships of opportunity," *Journal of Atmospheric and Oceanic Technology*, vol. 31, no. 7, pp. 1564–1582, 2014.

[15] L. Washburn, E. Romero, C. Johnson, B. Emery, and C. Gotschalk, "Measurement of antenna patterns for oceanographic radars using aerial drones," *Journal of Atmospheric and Oceanic Technology*, vol. 34, no. 5, pp. 971–981, 2017.

[16] Y. Tian, B. Wen, Z. Li, Y. Yin, and W. Huang, "Analysis and validation of an improved method for measuring HF surface wave radar antenna pattern," *IEEE Antennas and Wireless Propagation Letters*, vol. 18, no. 4, pp. 659–663, 2019.

[17] R. Wang, B. Wen, and W. Huang, "A support vector regression-based method for target direction of arrival estimation from HF radar data," *IEEE Geoscience and Remote Sensing Letters*, vol. 15, no. 5, pp. 674–678, 2018.

[18] B. Lu, B. Wen, Y. Tian, and R. Wang, "Analysis and calibration of crossed-loop antenna for vessel DOA estimation in HF radar," *IEEE Antennas and Wireless Propagation Letters*, vol. 17, no. 1, pp. 42–45, 2018.

[19] P. Stoica and A. Nehorai, "MUSIC, maximum likelihood, and cramer-rao bound," *IEEE Transactions on Acoustics, Speech, and Signal Processing*, vol. 37, no. 5, pp. 720–741, 1989.

[20] Y. Tian, B. Wen, J. Tan, and Z. Li, "Study on pattern distortion and DOA estimation performance of crossed-loop/monopole antenna in HF radar," *IEEE Transactions on Antennas and Propagation*, vol. 65, no. 11, pp. 6095–6106, 2017.

[21] S. U. Pillai and B. H. Kwon, "Performance analysis of MUSIC-type high resolution estimators for direction finding in correlated and coherent scenes," *IEEE Transactions on Acoustics, Speech, and Signal Processing*, vol. 37, no. 8, pp. 1176–1189, 1989.

[22] T.-J. Shan, M. Wax, and T. Kailath, "On spatial smoothing for direction-of-arrival estimation of coherent signals," *IEEE Transactions on Acoustics, Speech, and Signal Processing*, vol. 33, no. 4, pp. 806–811, 1985.

[23] Y. Tian, B. Wen, J. Tan, K. Li, Z. Yan, and J. Yang, "A new fully-digital HF radar system for oceanographical remote sensing," *IEICE Electronics Express*, vol. 10, no. 14, 2013.

[24] H. Rohling, "Radar CFAR thresholding in clutter and multiple target situations," *IEEE Transactions on Aerospace and Electronic Systems*, vol. 19, no. 4, pp. 608–621, 1983.